



**University of
Zurich**^{UZH}

**Zurich Open Repository and
Archive**

University of Zurich
University Library
Strickhofstrasse 39
CH-8057 Zurich
www.zora.uzh.ch

Year: 2013

pH-dependent antibacterial effects on oral microorganisms through pure PLGA implants and composites with nanosized bioactive glass

Hild, Nora ; Tawakoli, Pune N ; Halter, Jonas G ; Sauer, Bärbel ; Buchalla, Wolfgang ; Stark, Wendelin J ; Mohn, Dirk

Abstract: Biomaterials made of biodegradable poly(-hydroxyesters) such as poly(lactide-co-glycolide) (PLGA) are known to decrease the pH in the vicinity of the implants. Bioactive glass (BG) is being investigated as a counteracting agent buffering the acidic degradation products. However, in dentistry the question arises whether an antibacterial effect is rather obtained from pure PLGA or from BG/PLGA composites, as BG has been proved to be antimicrobial. In the present study the antimicrobial properties of electrospun PLGA and BG45S5/PLGA fibres were investigated using human oral bacteria (specified with mass spectrometry) incubated for up to 24 h. BG45S5 nanoparticles were prepared by flame spray synthesis. The change in colony-forming units (CFU) of the bacteria was correlated with the pH of the medium during incubation. The morphology and structure of the scaffolds as well as the appearance of the bacteria were followed by microscopy. Additionally, we studied if the presence of BG45S5 had an influence on the degradation speed of the polymer. Finally, it turned out that the pH increase induced by the presence of BG45S5 in the scaffold did not last long enough to show a reduction in CFU. On the contrary, pure PLGA demonstrated antibacterial properties that should be taken into consideration when designing biomaterials for dental applications.

DOI: <https://doi.org/10.1016/j.actbio.2013.06.030>

Posted at the Zurich Open Repository and Archive, University of Zurich

ZORA URL: <https://doi.org/10.5167/uzh-86750>

Journal Article

Accepted Version

Originally published at:

Hild, Nora; Tawakoli, Pune N; Halter, Jonas G; Sauer, Bärbel; Buchalla, Wolfgang; Stark, Wendelin J; Mohn, Dirk (2013). pH-dependent antibacterial effects on oral microorganisms through pure PLGA implants and composites with nanosized bioactive glass. *Acta Biomaterialia*, 9(11):9118-9125.

DOI: <https://doi.org/10.1016/j.actbio.2013.06.030>

pH-dependent antibacterial effects on oral microorganisms through pure PLGA implants and composites with nano-sized bioactive glass

Nora Hild¹, Pune N. Tawakoli², Jonas G. Halter¹, Bärbel Sauer², Wolfgang Buchalla²,
Wendelin J. Stark¹, Dirk Mohn^{1,2*}

¹ Institute for Chemical and Bioengineering, Department of Chemistry and Applied Biosciences, ETH Zurich, 8093 Zurich, Switzerland

² Department of Preventive Dentistry, Periodontology, and Cariology, University of Zurich, Center of Dental Medicine, 8032 Zurich, Switzerland

(*) Corresponding author:

Dirk Mohn

Institute for Chemical and Bioengineering,
Department of Chemistry and Applied
Biosciences
ETH Zurich

Wolfgang-Pauli-Str. 10
8093 Zurich
Switzerland

Telephone: 0041 44 633 45 14

Fax: 0041 44 633 15 71

email: dirk.mohn@chem.ethz.ch

Department of Preventive Dentistry,
Periodontology and Cariology

University of Zurich, Center of
Dental Medicine

Plattenstr. 11
8032 Zurich
Switzerland

Abstract

Biomaterials made of biodegradable poly(α -hydroxyesters) like poly(lactide-*co*-glycolide) (PLGA) are known to decrease the pH in the vicinity of the implants. Bioactive glass (BG) is being investigated as a counteracting agent buffering the acidic degradation products. However, in dentistry the question arises whether an antibacterial effect is rather obtained from pure PLGA or from BG/PLGA composites, as BG has been proved antimicrobial. In the present study the antimicrobial properties of electrospun PLGA and BG45S5/PLGA fibres were investigated using human oral bacteria (specified with mass spectrometry) incubated for up to 24 h. BG45S5 nanoparticles were prepared by flame spray synthesis. The change in colony-forming units (CFU) of the bacteria was put into correlation with the pH of the medium during incubation. Morphology and structure of the scaffolds as well as the appearance of the bacteria were followed by microscopy. Additionally, we studied if the presence of BG45S5 had an influence on the degradation speed of the polymer. Finally, it turned out that the pH increase induced by BG45S5 presence in the scaffold did not last long enough to show a reduction in CFU. On the contrary, pure PLGA demonstrated antibacterial properties that should be taken into consideration when designing biomaterials for dental applications.

Key words: bioglass, implant, antimicrobial, electrospinning, nanoparticles

1. Introduction

Polymers and ceramics are two classes of materials that can be combined into porous, biodegradable and bioactive hybrids [1]. New biomaterials are designed to replace certain functions in the body and, thus, a vast field for biomedical composites in tissue engineering opens. Among synthetic polymers [2-4], poly(α -hydroxyesters) are most often used and are

very well investigated [5-7]. The copolymer poly(lactide-*co*-glycolide) (PLGA) approved by the Food and Drug Administration (FDA) is very promising as its properties may be tailored according to the ratio of the two constituents [5, 8]. Yet, PLGA lacks certain features, *e.g.* pH buffer effect, osteoinductivity, osteoconductivity, bioactivity, *etc.* that may be overcome by adding ceramics, to obtain a desired composite.

Ever since its introduction by Hench *et al.* in 1971 [9], bioactive glass (BG) offers great potential for biomedical applications. Next to its bone bonding feature, BG is also found to be antibacterial [10-12]. A most recent review by Jones highlights the commercial products using BG [11]. Boccaccini *et al.* summarised the beneficial properties of nanoscale BG, namely enhanced osteoconductivity compared to micron-sized material and the emerging possibilities for nanocomposites [13].

BG with various compositions (45S5 [14-20] or other [21-25]) have been mixed with PLGA to render the latter osteoconductive and in order to overcome the issue of inflammation responses caused by the acidic degradation by-products of PLGA. However, even if counterproductive in the orthopaedic field, one might think of the pH drop induced by PLGA as an antimicrobial tool useful in dentistry, especially, as this biomaterial design would function according to the same principle as the barrier put up by the stomach, which is known to be an effective obstacle for harmful bacteria [26].

To our best knowledge, among the different techniques used to produce BG-polymer composites [1, 11, 13], up to now, electrospinning has only been applied with sodium-free bioactive glass [27-34]. Usually, the electrospinning solution was obtained by mixing a sol-gel precursor of BG with a polymer solution. Bretcanu *et al.* and Yunos *et al.* electrospun their polymer onto BG45S5 pellets [35, 36], while in this study the BG45S5/PLGA composite was prepared by electrospinning a dispersion of the inorganic phase in the polymer solution. BG45S5 nanoparticles necessary to produce a stable dispersion for electrospinning were produced by flame spray synthesis.

The question remains whether electrospun PLGA or BG45S5/PLGA is a more effective disinfectant. This shall be clarified by studying the viability of human oral bacteria cultured on the two materials. The hypothesis of this study was that both scaffolds influence the viability of bacteria by a pH shift.

2. Materials and methods

2.1 Spherical, dispersible BG45S5 nanoparticles

Amorphous BG nanoparticles (BG45S5, 45.0 wt% SiO₂, 24.5 wt% Na₂O, 24.5 wt% CaO and 6.0 wt% P₂O₅) were prepared by flame spray synthesis according to a previously described procedure [37, 38]. Briefly, precursors of hexamethyldisiloxane (Acros Organics, Geel, Belgium, 98%), calcium-2-ethylhexanoic acid (AppliChem, Darmstadt, Germany, Ph. Eur. and Sigma-Aldrich, St Louis, USA, 99%), sodium-2-ethylhexanoic acid (Riedel-de Haën, Seelze, Germany, Ph. Eur. and Sigma-Aldrich, St Louis, USA, 99%) and tributyl phosphate (Sigma-Aldrich, St Louis, USA, 98%) were mixed accordingly. The mixture was diluted with tetrahydrofuran (THF, Fisher Scientific, Waltham, USA, unstabilised) at a volume ratio of 2:1, dispersed with oxygen (5 L min⁻¹) and fed (5 mL min⁻¹) through a capillary (diameter 0.4 mm) into a methane/oxygen flame. As formed BG nanoparticles (production rate: 25 g h⁻¹) were collected on metal filters and sieved (300 µm mesh) subsequently.

2.2 Nanocomposite scaffolds

PLGA (copolymer ratio of 85/15, Boehringer Ingelheim, Ingelheim am Rhein, Germany, Resomer Sample MD Type RG) was dissolved in chloroform (Sigma-Aldrich, St Louis, USA, Ph. Eur.). The electrospinning solution contained 6.5 wt% PLGA (referred to the total solution weight) and 5.0 wt% Tween20 (referred to the PLGA weight, Polysorbate20, Fluka Analytical, St Louis, USA, Ph. Eur.). During electrospinning the polymer solution was fed

with 4 mL h⁻¹ through a capillary (inner diameter = 1.0 mm) using the dry ice experimental set-up described elsewhere [39]. A high voltage of 20 kV was applied to the needle tip, which was kept in a chloroform/air stream [40]. The distance between the needle tip and the cylindrical collector (diameter = 8 cm, covered with aluminium foil) was kept at 20 cm. The cylindrical collector was filled completely with dry ice (~500 g). This allowed dry ice electrospinning for 75 consecutive minutes. The scaffolds were immediately stored under vacuum at room temperature (RT).

Electrospun scaffolds containing 30 wt% of BG45S5 nanoparticles were produced by first dispersing the corresponding amount of BG45S5 nanoparticles in a solution of THF and dimethylformamide (DMF, Sigma-Aldrich, St Louis, USA, Ph. Eur) by ultrasonication (Hielscher, Teltow, Germany, UP400S) for 5 min applying pulsed intervals (volume ratio THF:DMF = 3:1). Subsequently, PLGA was dissolved under stirring for 2 h at a concentration of 0.083 g mL⁻¹ with 3 wt% Tween20 (referred to the PLGA weight). Dry ice electrospinning was carried out at 20 kV with a distance of 15 cm and the dispersion being fed at 3 mL h⁻¹. No solvent/air stream was applied at the nozzle.

2.3 BG45S5 nanoparticles and scaffold characterisation

Transmission electron microscopy (TEM, FEI, Eindhoven, The Netherlands, Tecnai F30 ST) and Brunauer-Emmett-Teller (BET) surface area (Micromeritics, Norcross, USA, Tristar 3000) were used to characterise the BG45S5 nanoparticles. X-ray diffraction (XRD) patterns were collected on a X'Pert PRO-MPD (PANalytical, Almelo, The Netherlands, Cu K_α radiation, X'Celerator linear detector system, step size of 0.033°, ambient conditions).

The fibrous scaffolds were investigated by means of scanning electron microscopy (SEM, FEI, Eindhoven, The Netherlands, Nova NanoSEM 450, voltage 3-5 kV) after sputtering them with a 3 nm platinum layer (Leica Microsystems, Wetzlar, Germany, EM SCD005). The BG45S5 nanoparticle content was verified gravimetrically using a thermoanalyser (Linseis,

Selb, Germany, PT1600). The degradation of PLGA was determined after electrospinning (with or without BG45S5 nanoparticles). Additionally, the reduction of the molecular weight of PLGA in the course of anaerobic incubation of the electrospun scaffolds in medium (see section 2.4) at 37°C and 5% CO₂ for 2 weeks with regular medium change was followed. Electrospun scaffolds (50 ± 2 mg) were dissolved in THF and centrifuged ($21'500 \times g$, 10 min, Hitachi Koki, Tokyo, Japan, himac CT15E). The supernatant was taken and THF was evaporated at 60°C. The remaining PLGA was analysed with gel permeation chromatography (GPC, flow rate 1 mL min⁻¹, Viscotek TDA, Malvern, UK) using chloroform as eluting solvent. Pieces of the incubated scaffolds were taken to track morphological changes of the fibres by SEM after 3 washing steps in Millipore water.

2.4 pH evolution

50 ± 2 mg of electrospun pure PLGA and electrospun BG45S5/PLGA were immersed in 500 µL medium (400 µL NaCl solution (Braun, Melsungen, Germany, 0.9%) and 100 µL broth (standard nutrient broth I, Carl Roth, Karlsruhe, Germany, prepared according to manufacturer's instructions)). The pH change was assessed immediately after immersion without incubation using a pH meter (Mettler Toledo, Greifensee, Switzerland, FiveEasy, FE20). Subsequently, the scaffolds were incubated at 37°C and 5% CO₂ under anaerobic conditions and pH was measured after 0.25, 0.5, 1, 2, 4, 8 and 24 h ($n = 3$).

2.5 Oral bacteria experiments

2.5.1 Bacteria culture and viability

Prior to antibacterial experiments the electrospun scaffolds were sterilised by UV radiation (50 W m^{-2}) on both sides for 30 min. The antibacterial activity of the two types of electrospun scaffolds was investigated with bacteria from pooled saliva. The unstimulated saliva was collected from 14 volunteers over a period of 3 h (aged 26-50 years, with good oral health,

smokers and non-smokers). Samples were centrifuged (3 min, 1200 rpm, Eppendorf, Hamburg, Germany, Minispin) and supernatant was pooled afterwards by vortexing for 1 min. Broth with 15 vol% glycerol was added to the pooled saliva in equal ratio. The mixture was divided in 1 mL aliquots and stored at -20°C.

The scaffolds (50 ± 2 mg) were incubated with 50 μ L bacteria suspension, 50 μ L broth and 400 μ L NaCl solution. The bacteria suspension was gained by thawing aliquots of pooled saliva, followed by centrifugation (1 min, 3000 rpm) and resuspension in broth for 1h at 37°C and 5% CO₂. Afterwards, the incubation of bacteria with the scaffolds for 2 h or 24 h (separate tests) was carried out under anaerobic conditions at 37°C and 5% CO₂. After incubation, colony-forming units (CFU) per mL were assessed from 100 μ L bacterial suspension. The incubated suspension was vortexed, diluted in NaCl solution and cultured on Columbia blood agar plates (VWR, Radnor, USA). The threshold values determinable for log₁₀ CFU per mL were 2.0 at the minimum and 8.6 at the maximum. Furthermore, pH of the suspension after incubation was assessed. As references to the tubes incubated with the electrospun scaffolds, the solutions summarised in Table 1 were additionally measured. Again, 50 μ L bacteria suspension and 50 μ L broth were incubated with 400 μ L of the respective reference solution. In addition to CFU counted after 24 h for every reference, pure medium and BG45S5 nanoparticle dispersions were also tested after 2 h. Two test series were carried out with independently thawed aliquots. Per series each material and reference was tested in triplicate (overall $n = 6$).

Table 1. pH, concentration and preparation of the solutions serving as references for the bacteria culture experiments with PLGA and BG45S5/PLGA scaffolds.

reference	pH ^a	concentration	buffer adjusted with	name
NaCl solution	7.4	0.9%	dna ^b	medium
HCl (Sigma-Aldrich, St Louis, USA, 37%) in NaCl solution	1.9	50 mmol L ⁻¹	dna ^b	HCl
lactic acid buffer solution in NaCl solution made with sodium L-lactate (Sigma-Aldrich, St Louis, USA, 98%)	3.5	50 mmol L ⁻¹	HCl in NaCl solution	lactic acid
phosphate buffered saline (Invitrogen, Carlsbad, USA)	7.4	dna ^b	dna ^b	PBS
NaHCO ₃ (Fluka Analytical, St Louis, Ph. Eur.) buffer solution in NaCl solution	7.8	50 mmol L ⁻¹	HCl in NaCl solution	NaHCO ₃
NaOH (Merck, Darmstadt, Germany, Ph. Eur.) in NaCl solution	9.7	^c	NaCl solution	NaOH
TAPS ^d (Sigma-Aldrich, St Louis, USA, 99%) buffer solution in NaCl solution	9.9	50 mmol L ⁻¹	NaOH in NaCl solution	TAPS
BG45S5 particles	11.5	15 mg in 500 μ L medium	dna ^b	BG45S5 particles

^a initial pH of the solution before addition of broth and bacteria suspension

^b does not apply

^c 9 mmol L⁻¹ NaOH in NaCl solution adjusted to pH with NaCl solution

^d 3-[N-Tris-(hydroxymethyl)methylamino]-2-hydroxypropanesulphonic acid

2.5.2 Bacteria and scaffold imaging

Confocal laser scanning microscopy (CLSM, Leica Microsystems, Wetzlar, Germany, SP5) was used to determine the bacteria viability qualitatively and to determine their appearance in the fibrous mesh. After incubation, the sample was vortexed and the medium was subsequently aspirated from the scaffold. Then, the PLGA or BG45S5/PLGA scaffolds were

washed in NaCl solution, fixed with 4% paraformaldehyde in the dark at RT for 60 min and washed once more with NaCl solution. LIVE/DEAD BacLight staining was used according to the manufacturer's instructions (Invitrogen, Carlsbad, USA). To that effect, stock solution A and B were mixed in equal ratios. After staining, the scaffolds were attached onto glass slides with the help of Mowiol (Sigma-Aldrich, St Louis, USA). Curing took 6 h in the dark. Images were taken with a 63 × (glycerol immersion, numerical aperture: 1.3) objective and an Argon, Helium, Neon laser with excitation/emission maxima of 488/500 nm and 561/635 nm using fluorescein isothiocyanate and TexasRed fluorescence filters. Each sample was examined by taking at least one stack with z step size < 1 μm. Image processing was performed with Imaris Software (Bitplane Scientific Software 7.5.1) after deconvolution using Huygens Remote Manager (Scientific Volume Imaging B.V. 2.1.2).

For SEM, the scaffolds were washed with NaCl solution and fixed in 10 wt% glutaraldehyde solution (Sigma-Aldrich, St Louis, USA, 25%) for 30 min. Dehydration was achieved gradually (2 × 15 min in ethanol 50 vol%, 2 × 15 min in ethanol 70 vol%, 2 × 15 min in ethanol 80 vol%, 2 × 15 min in ethanol 90%, 3 × 20 min and 2 × 60 min in ethanol absolute, Scharlau Chemie, Sentmenat, Spain, Ph. Eur.).

2.5.3 Bacteria identification

Bacteria species were determined with the help of mass spectrometric methods by Mabritec AG (Riehen, Switzerland). Four different samples were analysed in terms of species presence: the inoculum and samples incubated for 24 h at 37°C and 5% CO₂ under anaerobic conditions in pure medium or with PLGA or BG45S5/PLGA (*n* = 3).

2.6 Statistical analysis

The results of the CFU counting were obtained by \log_{10} -transformation of the values. The so-obtained values of the samples were normalised to the respective inoculum value (2 separate aliquots from the same pool) and are expressed as average \pm standard deviation of the mean. Statistical significance was evaluated by one-way ANOVA with Bonferroni correction. Statistical significance was accepted at $p < 0.05$.

3. Results and discussion

3.1 Spherical, dispersible BG45S5 nanoparticles

Brunauer-Emmet-Teller (BET) measurement of the BG45S5 nanoparticles gave a specific surface area of $40 \pm 4 \text{ m}^2 \text{ g}^{-1}$ corresponding to a primary particle diameter of 60 nm if the particles are assumed to be spherical. As shown in Figure S1, TEM supported the assumption of spherical particles and showed similar particles as those presented in previous publications [37, 38]. XRD pattern confirmed the BG45S5 nanoparticles to be XRD-amorphous (data not shown).

3.2 Nanocomposite scaffolds

Scaffolds made of pure PLGA or composed of BG45S5 nanoparticles and PLGA were prepared by electrospinning. Thermogravimetric analysis of the electrospun scaffolds containing BG45S5 nanoparticles confirmed that the nominal content of 30 wt% was achieved ($29 \pm 3 \text{ wt\%}$, $n = 16$). SEM micrographs of as prepared electrospun scaffolds are shown in Figure 1. The average fibre diameter ($n = 100$) of the pure PLGA fibres was $4990 \pm 810 \text{ nm}$ compared to $520 \pm 160 \text{ nm}$ for BG45S5/PLGA fibres. The diameter of pure PLGA fibres was in agreement with data published earlier [39, 41-43]. On the other hand, the smaller diameter of the BG45S5/PLGA fibres might have several causes. Most importantly, BG45S5-

containing fibres were electrospun from a different solvent system. The morphological appearance of the fibres was similar to that obtained by Dinarvand *et al.* [28].

Figure 2a summarises the GPC results. As anticipated, the presence of bioactive glass caused slightly faster degradation during incubation with medium. The electrospinning process resulted in a material with weight average molecular weight that was in the same range as extruded PLGA and slightly below solvent casted PLGA [44].

SEM micrographs of the immersed scaffolds proved that the morphology of the pure PLGA fibres did not change over incubation time (Figure S2 in the Supplementary data). However, it seemed as if the mesh was denser. In the case of BG45S5/PLGA, the fibrous morphology was lost (Figure S2 in the Supplementary Data). Crystallites demonstrating the mineralisation of the material were not as clearly visible as in *in vitro* studies with bioactive glasses (45S5 composition) in SBF or PBS [36, 37, 45], as neither calcium nor phosphate ions were present in the here applied incubation medium. However, it is legitimate to hypothesise the presence of apatite on the fibres as confirmed by Gubler *et al.* with corresponding Raman peaks when using the same BG nanoparticles in the same immersion medium (NaCl) [46].

3.3 pH evolution

The influence of the presence of BG45S5 in the PLGA fibres on the pH is depicted in Figure 2b. Compared to results reported in literature [14, 17, 22, 25] using PLGA with different L/G ratio and processed with other methods, in our case the pH drop caused by PLGA was more pronounced. For one, part of the mentioned studies examined the pH evolution in buffered solutions. Secondly, as bacteria culture conditions with 5% CO₂ and under anaerobic atmosphere favour a pH decrease, the acidity increased within 24 h in our case. BG45S5 buffers the pH decrease induced by the presence of PLGA. As a matter of fact, in literature it is often suggested to revert to orthopaedic implants made of PLGA and BG45S5 in order to avoid immune reactions like inflammations [1, 14, 17, 25].

From the opposite point of view, the antimicrobial effect of BG45S5 (nano-)particles is based on the pH increase that they induce [10, 46, 47], in addition to an ion release effect [46]. 15 mg of BG45S5 nanoparticles in 500 μ L medium caused the pH to rise to 11.5 (see Table 1) and after 24 h incubation at 37°C and 5% CO₂ the solution still presented a pH of 9.3 (see Table 2, below). If compared to previous studies using micron-sized BG and a more buffered medium, these values were slightly higher [48]. As expected, 50 mg of BG45S5/PLGA electrospun fibres provoked, in the same amount of medium a more moderate elevation of the pH (10.1, Figure 2b). After incubation for 24 h the pH dropped to 7.8 (Figure 2b).

3.4 Oral bacteria experiments

3.4.1 Bacteria culture and viability

In the following, the antimicrobial effect of the two materials was evaluated in order to determine which of them offered the more promising features to be used in dental applications. Hence a pool of mixed bacteria was investigated. Figure 3 illustrates the evolution of the bacteria viability. The reference in pure medium confirmed that bacteria had enough nutrients to grow (\log_{10} CFU per mL of the inoculum: ~ 6.8 , after 2 h: ~ 6.0 and after 24 h: ~ 6.6). In comparison, BG45S5 nanoparticles completely killed all bacteria within 24 h. This result is in agreement with previous studies. Similar to BG45S5 nanoparticles, the electrospun BG45S5/PLGA fibres initially showed an antimicrobial effect after 2 h. However, it seems that the composite material neither raised the pH enough nor did it keep the pH sufficiently long at elevated levels to kill all the bacteria. After 24 h the bacteria had recovered completely. In addition to this apparently too short pH rise, the increased viability after 24 h compared to culture in pure medium implies that the BG45S5 (phosphate-containing) acts as an additional nutrient source. On the other hand, PLGA electrospun fibres do not present a statistically significant influence on bacterial viability if compared to pure medium at first (2 h). Yet, after 24 h the CFU dropped significantly. To our best knowledge

the antimicrobial properties of PLGA have been studied only as a reference to scaffolds containing drugs [49, 50]. Unfortunately, in both cases, a different L/G ratio and combinations with other polymers do not allow a direct comparison to be drawn to our results.

Table 2 gives an overview on the evolution of the pH and puts it in context with the CFU results. High CFU counts after 24 h were observed for the solutions presenting a pH between 4 and 8 after incubation which is consistent with literature [51]. The disinfectant effect of HCl and the lactic acid buffered solution goes along with the results of Zhu *et al.* on *E. coli* and *H. pylori* [26]. PLGA brought the pH in the same range during incubation, which explains the CFU decline. The decrease in pH resulted in a stress-induced killing of bacteria. Only aciduric strains could survive, proliferate selectively and become dominant (see section 3.4.3).

Allan *et al.* [10] stated the antibacterial effect of bioactive glass as a phenomenon related to the alkaline nature of its surface reactions. However, in this study the fibrous material somehow encapsulated the particles and, thus, released its allegedly antibacterial effect more slowly than mere BG particles. Compared to incubation with pure PLGA, bacterial incubation with BG45S5/PLGA fibers gave higher bacteria counts and higher diversity of bacterial species (see section 3.4.3). Hence, combination of BG45S5 and PLGA prevented the pH to increase enough to reach pH levels with an ultimate antibacterial effect after 24 h.

TAPS buffer raised the pH to a similar level as BG45S5/PLGA fibres after 24 h. As a matter of fact, CFU were even uncountable after incubation in TAPS buffer. This confirmed the insufficiently high pH increase with creation of an enhanced bacteria friendly pH-environment.

Consequently, biomaterial properties can be modified and designed to embrace specific applications by adjusting the BG45S5 content in *e.g.* poly(α -hydroxyesters). Concerns regarding negative influences of the pH shift may rise [52]. Especially, a persistent pH decrease would make further investigations necessary in order to exclude severe long-term effects on the periodontal tissue. However, it can be assumed that the use of PLGA is unproblematic as it is already used in commercially available products for periodontal regeneration [53]. Table 2. pH after 24 h of incubation at 37°C and 5% CO₂ under anaerobic conditions with or without bacteria. Bacteria viability is expressed by means of CFU normalised to the CFU of the inoculum. In the case of bacteria culture in NaHCO₃ and TAPS

buffer, the dilutions were not sufficiently high to obtain countable amount of CFU on the agar plates (\log_{10} CFU per mL > 8.6) Same letters behind the value indicate no statistically significant difference.

	pH after 24 h without bacteria (<i>n</i> = 2)	pH after 24 h with bacteria (<i>n</i> = 6)	CFU after 24 h normalised to initial CFU (<i>n</i> = 6)
PLGA	3.8 ± 0.2	3.6 ± 0.1	0.57 ± 0.17
BG45S5/PLGA	7.9 ± 0.3	8.0 ± 0.1	1.09 ± 0.08, a
NaCl	5.8 ± 0.1	4.4 ± 0.2	0.97 ± 0.19, a
HCl	2.6 ± 0.1	2.6 ± 0.1	no CFU, b
lactic acid	3.7 ± 0.1	3.7 ± 0.1	no CFU, b
PBS	6.4 ± 0.2	5.3 ± 0.4	1.01 ± 0.06, a,c
NaHCO ₃	7.5 ± 0.3	7.6 ± 0.1	not determinable
NaOH	6.0 ± 0.1	4.6 ± 0.1	0.87 ± 0.05, c
TAPS	7.4 ± 0.1	7.4 ± 0.1	not determinable
BG45S5 particles	9.3 ± 0.1	9.5 ± 0.5	no CFU, b

3.4.2 Bacteria and scaffold imaging

On CLSM images (Figure 4), dead bacteria appeared red while living bacteria were green. Indeed, the differentiation of living and dead bacteria was possible. For PLGA, most bacteria were found at the scaffolds' border whereas BG45S5/PLGA scaffolds presented a distribution of living and dead bacteria throughout the fibrous mesh. The structure of the PLGA scaffolds looked loose and more porous in comparison with the entangled morphology of the BG45S5/PLGA scaffolds. This observation was confirmed by SEM.

Pure PLGA electrospun fibres presented the same morphology after 24 h bacteria culture as fibres incubated for 2 weeks without bacteria (Figure S2). Bacteria were found neither after 2 h nor after 24 h. After all, as CLSM had already shown, the bacteria were less embedded in the PLGA scaffolds compared to the BG45S5/PLGA mesh. Moreover, vortexing might have caused removal of the bacteria from the scaffolds to a certain degree. On the contrary, BG45S5/PLGA allowed observation of bacteria (Figure 5). After 24 h bacteria were spotted in the fibrous web. Similarly to CLSM images, bacteria appeared accumulated in certain parts of the scaffolds and were not homogeneously distributed over the scaffold.

3.4.3 Bacteria identification

Bacteria identification with the help of mass spectrometry was carried out for the inoculum and samples where bacteria were incubated for 24 h in pure medium or with PLGA or BG45S5/PLGA. The results are summarised in Table 3. Various *Streptococcus* species were present in the inoculum. These are typically found in the oral cavity [54]. It is noteworthy that after incubation with BG45S5/PLGA neither *Streptococcus parasanguinis* nor *Streptococcus mitis/oralis/pseudopneumoniae* were identified. As for PLGA, if CFU formed, only *Lactobacillus paracasei* was determined (2 samples did not present any CFU). This strain is most probably also present in the inoculum but is overgrown by the *Streptococci*. It is not surprising that *Lactobacillus paracasei* is the only species found after incubation with PLGA, as the *Lactobacillus* genus is known to grow best in slightly acidic media with initial pH of 6.4 – 4.5. Its growth is optimal under anaerobic conditions possibly stimulated with increased CO₂ concentration (5%) and ceases when pH 4.0 – 3.6 is reached [55].

Table 3. Qualitative identification of the bacteria. Besides inoculum, samples incubated for 24 h at 37°C and 5% CO₂ under anaerobic conditions either in pure medium or with PLGA or with BG45S5/PLGA were tested ($n = 3$). If the bacteria species was identified by mass spectrometry a plus (+) is noted. A minus (–) is noted when the species was not detected.

bacteria species	inoculum	medium	PLGA	BG45S5/PLGA
<i>Streptococcus parasanguinis</i>	+	+	-	-
<i>Streptococcus mitis/oralis/pseudopneumoniae</i>	+	+	-	-
<i>Streptococcus sp.</i>	-	+	-	+
<i>Streptococcus gordonii</i>	+	-	-	+
<i>Streptococcus sanguinis</i>	+	-	-	+
<i>Streptococcus sp. / cristatus</i>	-	-	-	+
<i>Streptococcus salivarius</i>	+	+	-	+
<i>Lactobacillus paracasei</i>	-	-	+	-
no CFU	-	-	+	-

4. Conclusion

Antimicrobial properties of electrospun PLGA and PLGA with BG45S5 nanoparticles were investigated. The evolution of CFU of human oral bacteria was brought into association with the pH shift of the medium induced by the scaffolds. It can be concluded that even if advantageous in orthopaedics the buffering effect of BG45S5 in polymeric composites prevents disinfection in dental applications. This shows that the optimal biomaterial design has to be adapted on the targeted function.

Acknowledgements

The authors would like to thank Dr. Thomas Schweizer for help with GPC measurement, Dr. Inge Herrmann for statistical analyses, Philipp Stössel for assistance with SEM and Dr. José María Mateos Melero for support with CLSM. Financial support by the authors' institutions is kindly acknowledged.

References

- [1] Rezwan K, Chen QZ, Blaker JJ, Boccaccini AR. Biodegradable and bioactive porous polymer/inorganic composite scaffolds for bone tissue engineering. *Biomaterials* 2006;27:3413-3431.
- [2] Agrawal CM, Ray RB. Biodegradable polymeric scaffolds for musculoskeletal tissue engineering. *J Biomed Mater Res* 2001;55:141-150.
- [3] Barrows TH. Degradable implant materials: a review of synthetic absorbable polymers and their applications. *Clin Mater* 1986;1:233-257.
- [4] Hutmacher DW. Scaffolds in tissue engineering bone and cartilage. *Biomaterials* 2000;21:2529-2543.
- [5] Agrawal CM, Niederauer GG, Micallef DM, Athanasiou KA. The Use of PLA-PGA Polymers in Orthopedics. In: Wise DL, Trantolo DJ, Altobelli DE, Yaszemski MJ, Gresser JD, Schwartz ER, editors. *Encyclopedic Handbook of Biomaterials and Bioengineering Part A: Materials*. 1st ed. New York, NY: Marcel Dekker, Inc.; 1995. p. 1055-1089.
- [6] Athanasiou KA, Agrawal CM, Barber FA, Burkhart SS. Orthopaedic applications for PLA-PGA biodegradable polymers. *Arthroscopy* 1998;14:726-737.
- [7] Middleton JC, Tipton AJ. Synthetic biodegradable polymers as orthopedic devices. *Biomaterials* 2000;21:2335-2346.

- [8] Anderson JM, Shive MS. Biodegradation and biocompatibility of PLA and PLGA microspheres. *Adv Drug Deliver Rev* 1997;28:5-24.
- [9] Hench LL, Splinter RJ, Allen WC, Greenlee TK. Bonding mechanisms at the interface of ceramic prosthetic materials. *J Biomed Mater Res* 1971;5:117-141.
- [10] Allan I, Newman H, Wilson M. Antibacterial activity of particulate Bioglass (R) against supra- and subgingival bacteria. *Biomaterials* 2001;22:1683-1687.
- [11] Jones JR. Review of bioactive glass: From Hench to hybrids. *Acta Biomater* 2013;9:4457-4486.
- [12] Stoor P, Soderling E, Salonen JI. Antibacterial effects of a bioactive glass paste on oral microorganisms. *Acta Odontol Scand* 1998;56:161-165.
- [13] Boccaccini AR, Erol M, Stark WJ, Mohn D, Hong Z, Mano JF. Polymer/bioactive glass nanocomposites for biomedical applications: A review. *Compos Sci Technol* 2010;70:1764-1776.
- [14] Boccaccini AR, Maquet V. Bioresorbable and bioactive polymer/Bioglass (R) composites with tailored pore structure for tissue engineering applications. *Compos Sci Technol* 2003;63:2417-2429.
- [15] Day RM, Maquet V, Boccaccini AR, Jerome R, Forbes A. In vitro and in vivo analysis of macroporous biodegradable poly(D,L-lactide-co-glycolide) scaffolds containing bioactive glass. *J Biomed Mater Res Part A* 2005;75A:778-787.
- [16] Keshaw H, Georgiou G, Blaker JJ, Forbes A, Knowles JC, Day RM. Assessment of Polymer/Bioactive Glass-Composite Microporous Spheres for Tissue Regeneration Applications. *Tissue Eng Part A* 2009;15:1451-1461.
- [17] Li HY, Chang J. pH-compensation effect of bioactive inorganic fillers on the degradation of PLGA. *Compos Sci Technol* 2005;65:2226-2232.
- [18] Lu HH, El-Amin SF, Scott KD, Laurencin CT. Three-dimensional, bioactive, biodegradable, polymer-bioactive glass composite scaffolds with improved mechanical

- properties support collagen synthesis and mineralization of human osteoblast-like cells in vitro. *J Biomed Mater Res Part A* 2003;64A:465-474.
- [19] Yao J, Radin S, Leboy PS, Ducheyne P. The effect of bioactive glass content on synthesis and bioactivity of composite poly (lactic-co-glycolic acid)/bioactive glass substrate for tissue engineering. *Biomaterials* 2005;26:1935-1943.
- [20] Yao J, Radin S, Reilly G, Leboy PS, Ducheyne P. Solution-mediated effect of bioactive glass in poly (lactic-co-glycolic acid)-bioactive glass composites on osteogenesis of marrow stromal cells. *J Biomed Mater Res Part A* 2005;75A:794-801.
- [21] Orava E, Korventausta J, Rosenberg M, Jokinen M, Rosling A. In vitro degradation of porous poly(DL-lactide-co-glycolide) (PLGA)/bioactive glass composite foams with a polar structure. *Polym Degrad Stabil* 2007;92:14-23.
- [22] Pamula E, et al. Degradation, Bioactivity, and Osteogenic Potential of Composites Made of PLGA and Two Different Sol-Gel Bioactive Glasses. *Ann Biomed Eng* 2011;39:2114-2129.
- [23] Zhou Z, Gao Y, Yi Q, Liu Q, Liu L. Study on the Cytotoxicity In-vitro of Composite Materials Based on Poly(L-lactide-co-glycolide) and Bioactive Glass. *Mater Sci Forum* 2011;685:384-389.
- [24] Chen J, Fan X, Zhou Z, Zou J, Ruan J. The Preparation and Properties of Bioactive Composites Based on Modification Bioactive Glass and Poly(Lactide-Co-Glycolide). *Polym-Plast Technol* 2010;49:1155-1162.
- [25] Wu C, Ramaswamy Y, Zhu Y, Zheng R, Appleyard R, Howard A, Zreiqat H. The effect of mesoporous bioactive glass on the physiochemical, biological and drug-release properties of poly(DL-lactide-co-glycolide) films. *Biomaterials* 2009;30:2199-2208.
- [26] Zhu H, Hart CA, Sales D, Roberts NB. Bacterial killing in gastric juice - effect of pH and pepsin on *Escherichia coli* and *Helicobacter pylori*. *J Med Microbiol* 2006;55:1265-1270.

- [27] Allo BA, Rizkalla AS, Mequanint K. Synthesis and Electrospinning of epsilon-Polycaprolactone-Bioactive Glass Hybrid Biomaterials via a Sol-Gel Process. *Langmuir* 2010;26:18340-18348.
- [28] Dinarvand P, et al. New Approach to Bone Tissue Engineering: Simultaneous Application of Hydroxyapatite and Bioactive Glass Coated on a Poly(L-lactic acid) Scaffold. *ACS Appl Mater Interfaces* 2011;3:4518-4524.
- [29] Gao C, Gao Q, Bao X, Li Y, Teramoto A, Abe K. Preparation and In Vitro Bioactivity of Novel Mesoporous Borosilicate Bioactive Glass Nanofibers. *J Am Ceram Soc* 2011;94:2841-2845.
- [30] Kim H-W, Kim H-E, Knowles JC. Production and potential of bioactive glass nanofibers as a next-generation biomaterial. *Adv Funct Mater* 2006;16:1529-1535.
- [31] Kim H-W, Lee H-H, Chun G-S. Bioactivity and osteoblast responses of novel biomedical nanocomposites of bioactive glass nanofiber filled poly(lactic acid). *J Biomed Mater Res Part A* 2008;85A:651-663.
- [32] Kim IA, Rhee S-H. Effects of poly(lactic-co-glycolic acid) (PLGA) degradability on the apatite-forming capacity of electrospun PLGA/SiO₂-CaO nonwoven composite fabrics. *J Biomed Mater Res Part B* 2010;93B:218-226.
- [33] Lu H, Zhang T, Wang XP, Fang QF. Electrospun submicron bioactive glass fibers for bone tissue scaffold. *J Mater Sci-Mater M* 2009;20:793-798.
- [34] Xia W, Zhang D, Chang J. Fabrication and in vitro biomineralization of bioactive glass (BG) nanofibres. *Nanotechnology* 2007;18:135601-135607.
- [35] Bretcanu O, et al. Electrospun nanofibrous biodegradable polyester coatings on Bioglass (R)-based glass-ceramics for tissue engineering. *Mater Chem Phys* 2009;118:420-426.
- [36] Yunos DM, Ahmad Z, Boccaccini AR. Fabrication and characterization of electrospun poly-DL-lactide (PDLA) fibrous coatings on 45S5 Bioglass (R) substrates for bone tissue engineering applications. *J Chem Technol Biot* 2010;85:768-774.

- [37] Brunner TJ, Grass RN, Stark WJ. Glass and bioglass nanopowders by flame synthesis. *Chem Commun* 2006, 10.1039/b517501a.1384-1386.
- [38] Mohn D, Zehnder M, Imfeld T, Stark WJ. Radio-opaque nanosized bioactive glass for potential root canal application: evaluation of radiopacity, bioactivity and alkaline capacity. *Int Endod J* 2010;43:210-217.
- [39] Simonet M, Schneider OD, Neuenschwander P, Stark WJ. Ultraporous 3D polymer meshes by low-temperature electrospinning: Use of ice crystals as a removable void template. *Polym Eng Sci* 2007;47:2020-2026.
- [40] Larsen G, Spretz R, Velarde-Ortiz R. Use of coaxial gas jackets to stabilize Taylor cones of volatile solutions and to induce particle-to-fiber transitions. *Adv Mater* 2004;16:166-169.
- [41] Hild N, et al. Two-layer membranes of calcium phosphate/collagen/PLGA nanofibres: in vitro biomineralisation and osteogenic differentiation of human mesenchymal stem cells. *Nanoscale* 2011;3:401-409.
- [42] Schneider OD, et al. Cotton wool-like nanocomposite biomaterials prepared by electrospinning: In vitro bioactivity and osteogenic differentiation of human mesenchymal stem cells. *J Biomed Mater Res Part B* 2008;84B:350-362.
- [43] Hild N, Abächerli ML, Mohn D, Stark WJ. Heat-induced dry tailoring of porosity in polymer scaffolds. *Macromol Mater Eng* 2013, DOI: 10.1002/mame.201200327.
- [44] Mohn D, Ege D, Feldman K, Schneider OD, Imfeld T, Boccaccini AR, Stark WJ. Spherical Calcium Phosphate Nanoparticle Fillers Allow Polymer Processing of Bone Fixation Devices with High Bioactivity. *Polym Eng Sci* 2010;50:952-960.
- [45] Varila L, Fagerlund S, Lehtonen T, Tuominen J, Hupa L. Surface reactions of bioactive glasses in buffered solutions. *J Eur Ceram Soc* 2012;32:2757-2763.

- [46] Gubler M, Brunner TJ, Zehnder M, Waltimo T, Sener B, Stark WJ. Do bioactive glasses convey a disinfecting mechanism beyond a mere increase in pH? *Int Endod J* 2008;41:670-678.
- [47] Waltimo T, Brunner TJ, Vollenweider M, Stark WJ, Zehnder M. Antimicrobial effect of nanometric bioactive glass 45S5. *J Dent Res* 2007;86:754-757.
- [48] Sepulveda P, Jones JR, Hench LL. In vitro dissolution of melt-derived 45S5 and sol-gel derived 58S bioactive glasses. *J Biomed Mater Res* 2002;61:301-311.
- [49] Kim K, Luu YK, Chang C, Fang DF, Hsiao BS, Chu B, Hadjiargyrou M. Incorporation and controlled release of a hydrophilic antibiotic using poly(lactide-co-glycolide)-based electrospun nanofibrous scaffolds. *J Control Release* 2004;98:47-56.
- [50] Said SS, Aloufy AK, El-Halfawy OM, Boraei NA, El-Khordagui LK. Antimicrobial PLGA ultrafine fibers: Interaction with wound bacteria. *Eur J Pharm Biopharm* 2011;79:108-118.
- [51] Madigan MT, Martinko JM, Parker J. *Brock biology of microorganisms*. 8th ed. Upper Saddle River, NJ: Prentice-Hall International; 1997.
- [52] Blomlof J, Lindskog S. Periodontal tissue-vitality after different etching modalities. *J Clin Periodontol* 1995;22:464-468.
- [53] Bottino MC, Thomas V, Schmidt G, Vohra YK, Chu T-MG, Kowolik MJ, Janowski GM. Recent advances in the development of GTR/GBR membranes for periodontal regeneration-A materials perspective. *Dent Mater* 2012;28:703-721.
- [54] Hardy JM. Genus *Streptococcus*. In: Sneath PHA, Mair NS, Sharpe ME, Holt JG, editors. *Bergey's manual of systematic bacteriology*. Baltimore, MD: Williams & Wilkins; 1986. p. 1043-1071.
- [55] Kandler O, Weiss N. Genus *Lactobacillus*. In: Sneath PHA, Mair NS, Sharpe ME, Holt JG, editors. *Bergey's manual of systematic bacteriology*. Baltimore, MD: Williams & Wilkins; 1986. p. 1209-1234.

Figure Captions

Figure 1 Structure and morphology of as prepared scaffolds. Compared to the smooth PLGA fibres (a), the BG45S5 fibres presented nanoparticles at their surface (b).

Figure 2 Evolution of the molecular weight of PLGA in the scaffolds (a). Starting from as prepared scaffolds to scaffolds incubated at 37°C and 5% CO₂ under anaerobic conditions for 2 weeks, degradation was determined by GPC. Both scaffolds PLGA (Δ) and BG45S5/PLGA (\bullet) are shown. Evolution of the pH (b). The measurement started with pure medium (\times , 0 h) and the immediate pH change (0.05 h) induced by PLGA (Δ) or BG45S5/PLGA (\bullet) before incubation is shown. During incubation at 37°C and 5% CO₂ under anaerobic conditions starting at 1 h the pH decreased.

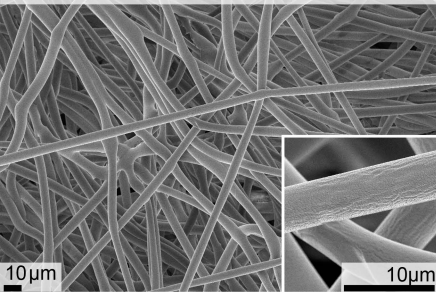
Figure 3 Evolution of CFU found in samples incubated for 2 h (left) or 24 h (right) at 37°C and 5% CO₂ under anaerobic conditions in pure medium, with PLGA, with BG45S5/PLGA or with BG45S5 particles ($n = 6$). A full disinfection was obtained with BG45S5 nanoparticles. It is noteworthy that the reduction of CFU after 24 h for bacteria incubated with PLGA is statistically significant as indicated ($p < 0.05$).

Figure 4 Appearance of the bacteria on the scaffolds by means of CLSM after cultivation for 24 h on PLGA (a, c, e) or on BG45S5/PLGA (b, d, f). Micrographs for channel 488/500 (a, b) and channel 561/635 (c, d) are shown separately and combined in an overlay (e, f). Living bacteria fluoresced green while dead bacteria emitted red fluorescence. On PLGA, the bacteria were found mostly at the scaffold's border as opposed to the broader distribution of

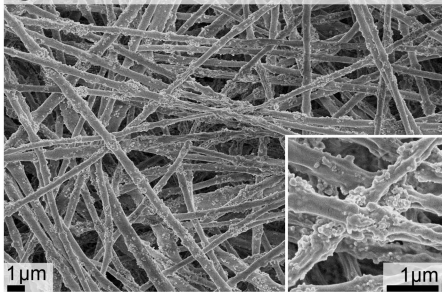
bacteria in the BG45S5/PLGA mesh. The PLGA fibres appeared loose in comparison with the entangled BG45S5/PLGA fibres.

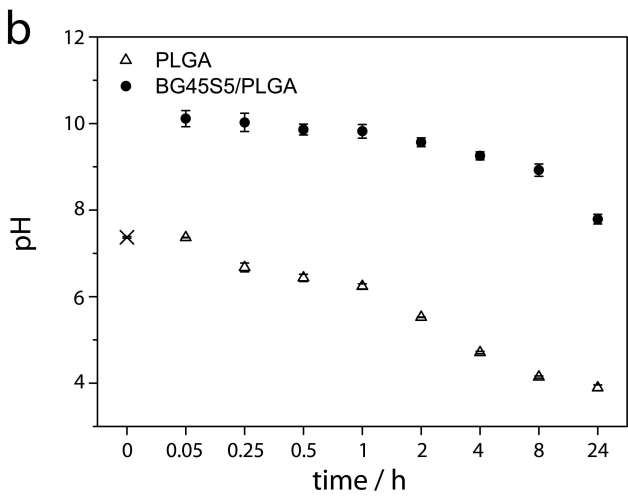
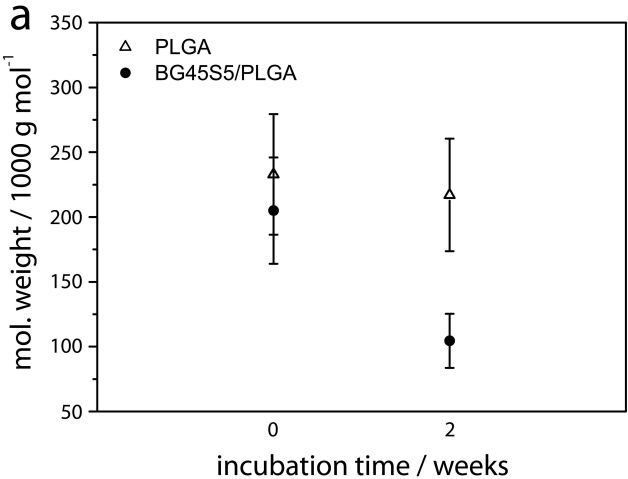
Figure 5 Structure and morphology of the scaffolds by means of SEM after BG45S5/PLGA were cultured for 2 h (a, b) or for 24 h (c, d) at 37°C and 5% CO₂ under anaerobic conditions with bacteria. SEM also showed bacteria on the scaffolds incubated for 24 h as indicated in (c) with arrows and magnified in (d).

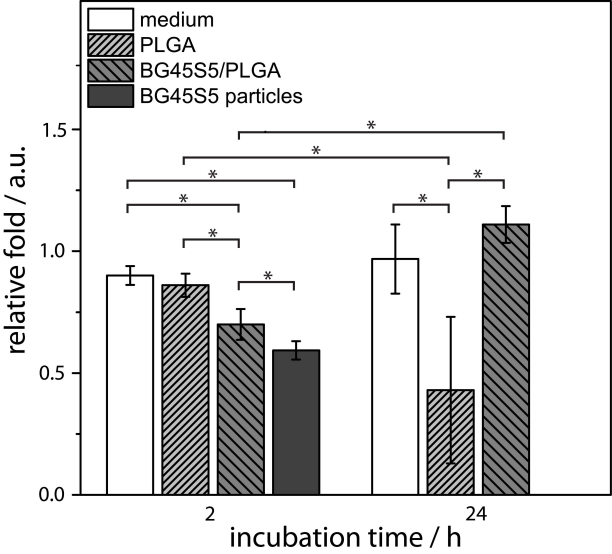
a PLGA; as prep.

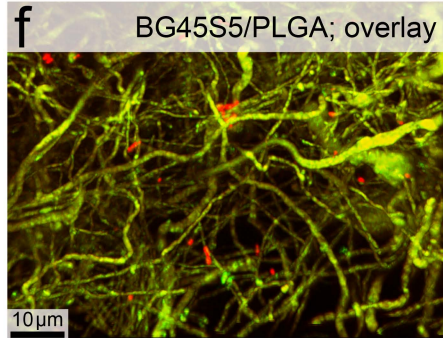
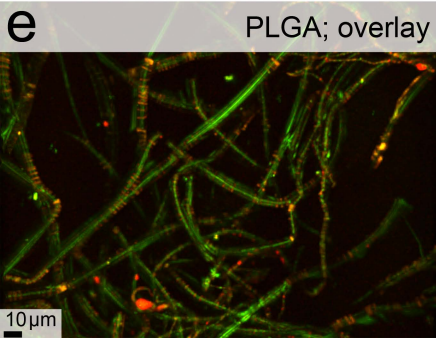
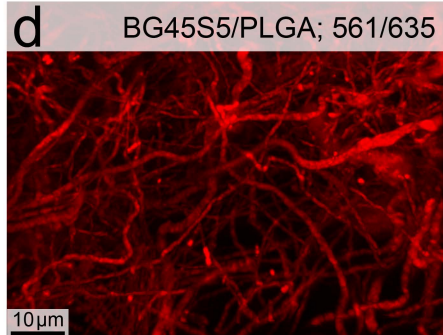
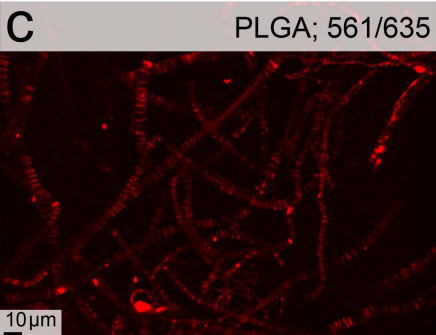
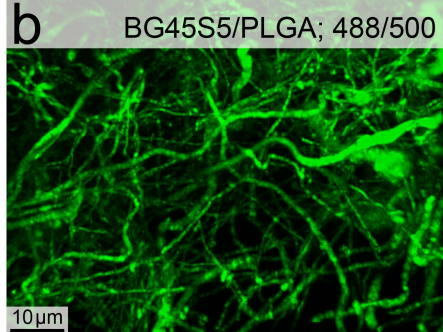
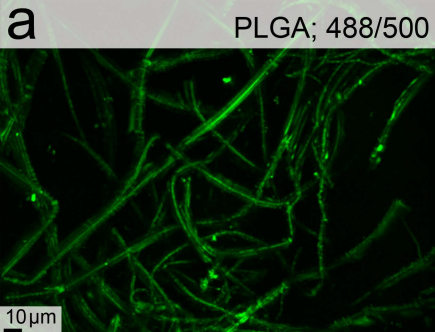


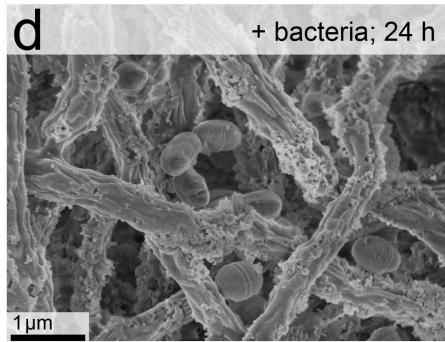
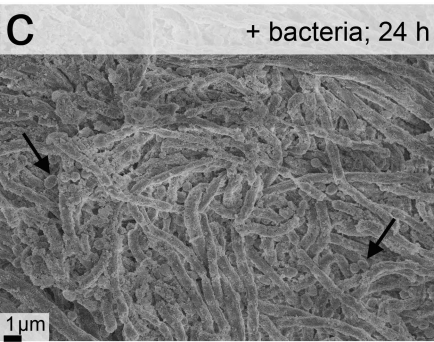
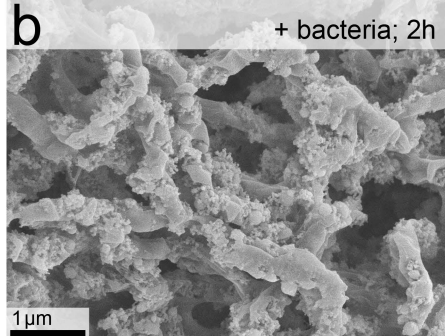
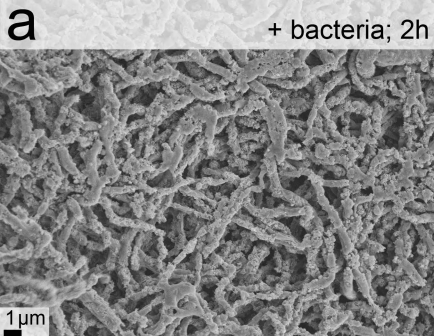
b BG45S5/PLGA; as prep.











Supplementary data

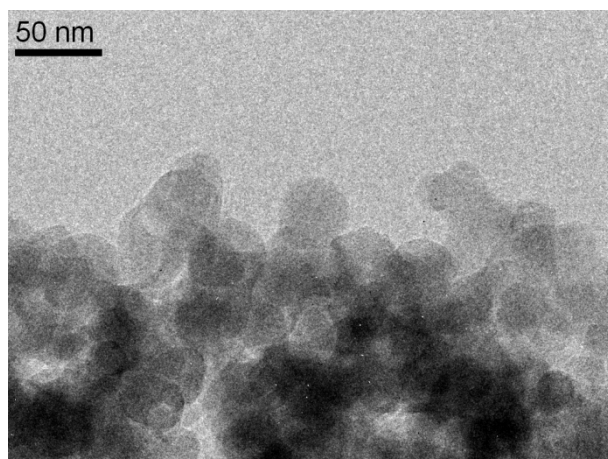


Figure S1 TEM of the flame spray-derived BG45S5 nanoparticles confirmed the spherical shape and the nano-size of the particles.

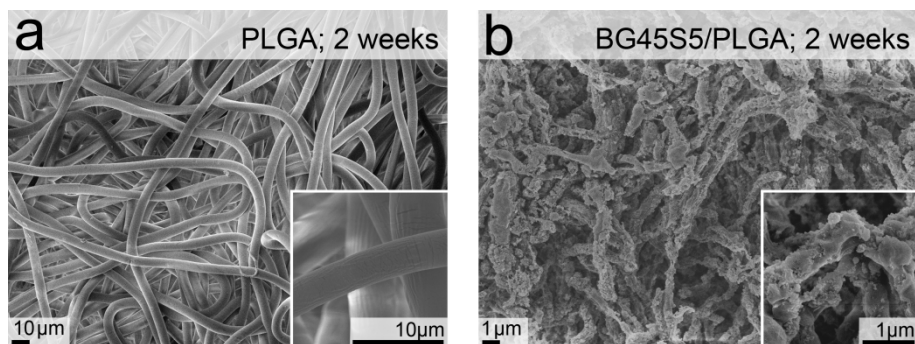


Figure S2 Structure and morphology of scaffolds incubated at 37°C and 5% CO₂ under anaerobic conditions for 2 weeks in pure medium. Pure PLGA fibres kept their morphology (a), whereas for BG45S5/PLGA scaffolds the fibrous mesh was mostly lost (b).